



# Interlobate esker aquifer characterization by high resolution seismic reflection method with landstreamer in SW Finland

Elina Ahokangas<sup>a,\*</sup>, Joni Mäkinen<sup>a</sup>, Aki Artimo<sup>b</sup>, Antti Pasanen<sup>c</sup>, Heikki Vanhala<sup>d</sup>

<sup>a</sup> University of Turku, Department of Geography and Geology, 20014 Turun yliopisto, Finland

<sup>b</sup> Turku Region Water Ltd, Maariankatu 1, 20100 Turku, Finland

<sup>c</sup> Geological Survey of Finland, P.O. Box 1237, 70211 Kuopio, Finland

<sup>d</sup> Geological Survey of Finland, P.O. Box 96, 02151 Espoo, Finland

## ARTICLE INFO

### Article history:

Received 15 August 2018

Received in revised form 2 April 2020

Accepted 6 April 2020

Available online 8 April 2020

### Keywords:

Interlobate esker

Aquifer

Characterization

High-resolution seismic method

Landstreamer

## ABSTRACT

The Virttaankangas interlobate esker with 100 m thick sediments has a complex depositional history. It is one of the largest groundwater reserves in Finland and hosts a managed artificial recharge plant providing potable water for the 300,000 inhabitants of the Turku region. We researched the characteristics of the esker aquifer both on a major fracture valley and on an esker ridge with a low groundwater table. This study presents the results of the first landstreamer-based high-resolution seismic reflection survey in Finland conducted in 2011. The esker core (main aquifer) position was delineated accurately throughout the entire area with continuous seismic data compared to a previous sedimentological model, gravimetric data and reference drillings. New features related to the widening of the coarse-grained unit of the esker core as well as a previously unknown daughter esker adjacent to the main esker core were revealed. These new findings are in agreement with the existing 3-D hydrogeological model. Our research provides valuable data on the high-resolution seismic reflection surveying of thick interlobate glaciofluvial deposits on two areas with differing bedrock topography on crystalline basement rocks.

© 2020 The Authors. Published by Elsevier B.V. This is an open access article under the CC BY license (<http://creativecommons.org/licenses/by/4.0/>).

## 1. Introduction

The main groundwater reserves in Finland are found in numerous glaciofluvial deposits (eskers) formed during the deglaciation of the Scandinavian Ice Sheet. Some exceptionally large eskers, like the Säköjärvi-Virttaankangas esker were deposited in an interlobate area between two ice lobes (Punkari, 1980; Kujansuu et al., 1995; Mäkinen, 2003a). Interlobate esker deposits can be up to 100 m thick and have varying sedimentary structures due to complex depositional conditions (Warren and Ashley, 1994; Brennand and Shaw, 1996; Thomas and Montaque, 1997; Russell et al., 2003; Sharpe et al., 2003; Gruszka et al., 2012; Santos, 2012; Ahokangas and Mäkinen, 2014). Therefore, the hydrogeological modeling and aquifer characterization of an interlobate complex and its large-scale architectural elements (e.g. highly hydraulically conductive esker cores) down to bedrock level could be advanced by the high-resolution seismic reflection method (HRSR). Ground penetrating radar (GPR) is an excellent tool

for the study of glaciofluvial deposits (cf. Mäkinen, 2003c; Sharpe et al., 2003; Burke et al., 2008; Pasanen, 2009), but its limited depth penetration (only 20–25 m) inhibits the characterization of the deeper parts of the interlobate deposits. The HRSR method with over 100 m depth penetration provides important information about the variations in bedrock topography and about continuities and thicknesses of sedimentary units, which control groundwater formation and flow patterns. Seismic interpretations of the sedimentary characteristics and environments can be used to estimate the continuities of different units outside the seismic profiles.

Seismic reflection surveying has been applied increasingly in engineering and environmental investigations since the 1980's (Steeple and Miller, 1990). The use of seismic landstreamers has become more frequent due to their cost-effectiveness and especially due to their suitability in near-surface investigations (Pugin et al., 2009a) and due to their efficiency in recording P- and S-wave data (Van der Veen et al., 2001; Inazaki, 2004; Vangkilde-Pedersen et al., 2006; Krawczyk et al., 2012; Pugin et al., 2013). The applications of HRSR with a landstreamer have mainly focused on the mapping of Quaternary deposits and on various hydrogeological studies of tunnel valley aquifers in USA and Canada (cf. Pugin et al., 1999; Pugin et al., 2004; Pullan et al., 2007; Pugin et al., 2009a, 2009b; Ahmad et al., 2009; Tremblay et al., 2010;

\* Corresponding author.

E-mail addresses: [eliah@utu.fi](mailto:eliah@utu.fi) (E. Ahokangas), [jonmak@utu.fi](mailto:jonmak@utu.fi) (J. Mäkinen), [aki.artimo@turunseudunvesi.fi](mailto:aki.artimo@turunseudunvesi.fi) (A. Artimo), [antti.pasanen@gtk.fi](mailto:antti.pasanen@gtk.fi) (A. Pasanen), [heikki.vanhala@gtk.fi](mailto:heikki.vanhala@gtk.fi) (H. Vanhala).

Oldenborger et al., 2013, 2016) and Northern Europe (Huuse et al., 2003; Kirsch et al., 2006; Martinez et al., 2010) as well as in esker characterization in Canada (Sharpe et al., 1992; Barnett et al., 1998; Pugin et al., 1999; Pullan et al., 2007; Cummings and Russell, 2007; Cummings et al., 2011), in Finland (Maries et al., 2017; Brodic et al., 2018) and in the Alpine range (Burschil et al., 2018). In addition, some landstreamer-based applications have been utilized in urban environments (Krawczyk et al., 2012; Brodic et al., 2015) and in the shallow subsurface imaging of transport routes (Pilecki et al., 2017; Malehmir et al., 2018).

The Virttaankangas aquifer hosts an artificial managed aquifer recharge (MAR) plant providing water for the 300,000 inhabitants of the Turku city region. Operation of the plant is based on a 3-D hydrogeological model containing the main hydrogeological units, identified based on a sedimentological model that was built from the sedimentological data combined with existing boreholes, GPR, gravimetric, and refraction seismic lines. This 3-D hydrogeological model (Artimo et al., 2003), integrated with a 60-layer groundwater flow model, is used as the tool in the management of the MAR plant (Artimo et al., 2008).

Our paper presents the first broad landstreamer-based HRSR application in Finland for the aquifer characterization of thick and extensive interlobate glaciofluvial deposits supported by abundant reference data from the MAR plant investigations. Our aim is to identify and characterize the deep parts of the Virttaankangas esker by seismic reflection data and to improve the 3-D hydrogeological model. The main objectives of this study are (1) to verify the location and architecture of the bouldery esker core (the main aquifer) in the investigated area, (2) to describe the sediment stratigraphy within the major fracture valley, and (3) to explain the widening of the coarse-grained hydrogeological unit where the main esker core is associated with tributary cores and a proposed crevasse deposits.

## 2. Study area

### 2.1. Geomorphological and geological background

The extensive interlobate Säkylänharju-Virttaankangas (SV) glaciofluvial complex in SW Finland (Fig. 1) is part of the hundreds of kilometers long Pori-Koski esker chain. The study area comprises Säkylänharju-Porsaanharju main ridge (up to 1 km wide and 40 m high) with the 5 km long, 2–4 km wide and 20–35 m high fan-like Virttaankangas plain in the southeast. The plain consists mostly of littorally reworked esker sediments (Mäkinen and Räsänen, 2003). Fine-grained varved glaciolacustrine deposits surround the esker and the plain (cf. Kukkonen et al., 1993) (Fig. 1a). The Löytäne tributary esker joins Virttaankangas from SW and discharges part of the groundwater towards the large Myllylähde spring south of the Virttaankangas plain (Fig. 1a).

The Virttaankangas plain has a varying bedrock topography and depositional characteristics as well as groundwater depths. It is located about 10 km southeast of the bedrock contact zone of the Satakunta sandstone depression and the Precambrian Svecofennian basement with igneous and metamorphic rocks (Hämäläinen, 1994), including quartz diorite, granodiorite with amphibolite, and intermediate gneiss (Salli, 1953a, 1953b). A major N-S oriented, 200–300 m wide and about 50 m deep fracture valley is buried beneath the Virttaankangas plain (Valjus, 2006) (Figs. 1, 2). It is plausible that there are unknown sandstone outliers within this fracture valley that are related to the major Satakunta sandstone depression ca. 15 km west of the study area (cf. Kaitanen and Ström, 1978). The sediment thicknesses in the study area are usually 20–60 m, but increase up to a 100 m in the fracture valley, where the stratigraphic characteristics are still poorly known. The bedrock level varies between –29–55 m in the fracture valley and between 55 and 95 m a.s.l. towards the Porsaanharju ridge (Valjus, 2006).

### 2.2. Sedimentological details and 3-D hydrogeological model of the Virttaankangas plain

The sedimentological studies, supplemented with GPR lines (cf. Fig. 1b), borehole logs, and gravimetric measurements, revealed the complexities of the Säkylänharju-Virttaankangas esker system (Artimo et al., 2003; Mäkinen, 2003c). The time-transgressively formed core of the interlobate esker is composed of repeated ice-marginal subaqueous fans fed by a subglacial meltwater tunnel. The fans show a transition from proximal gravels to medial large-scale foresets and finally to distal fine-grained glaciolacustrine deposits (Mäkinen, 2003c). In addition, the change in the depositional conditions of the esker led to the formation of interlobate ice-marginal crevasse deposits, which form the main Säkylänharju-Porsaanharju ridge.

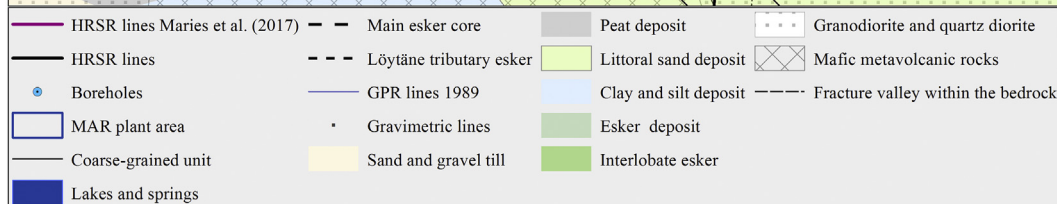
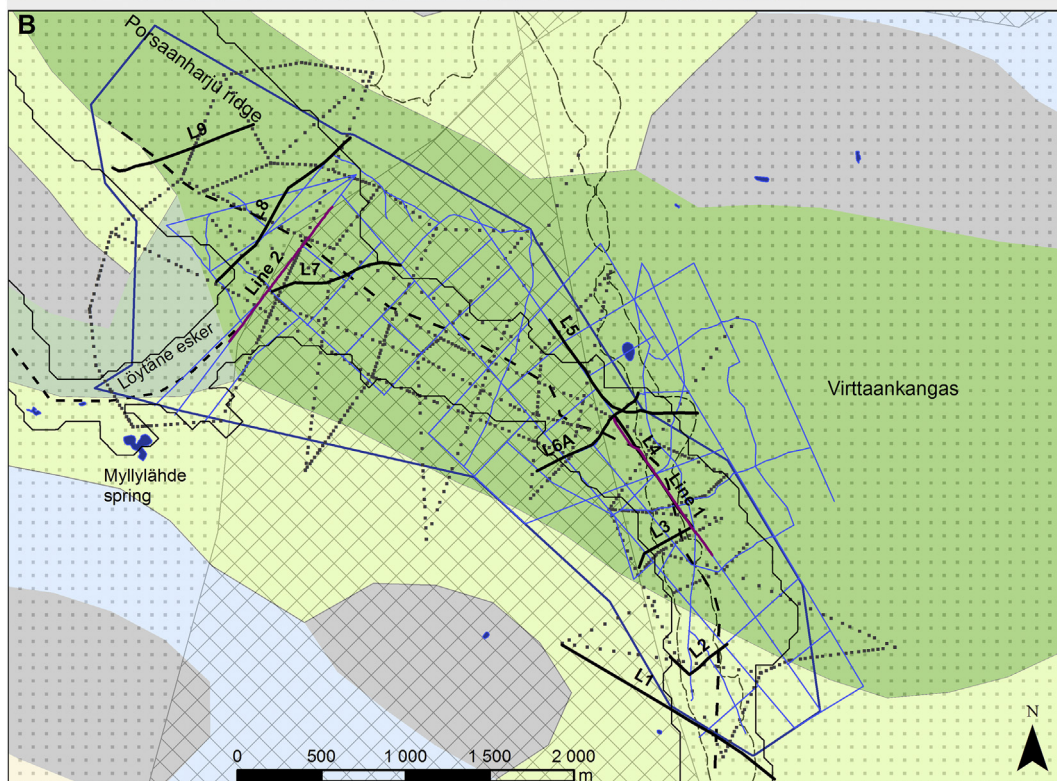
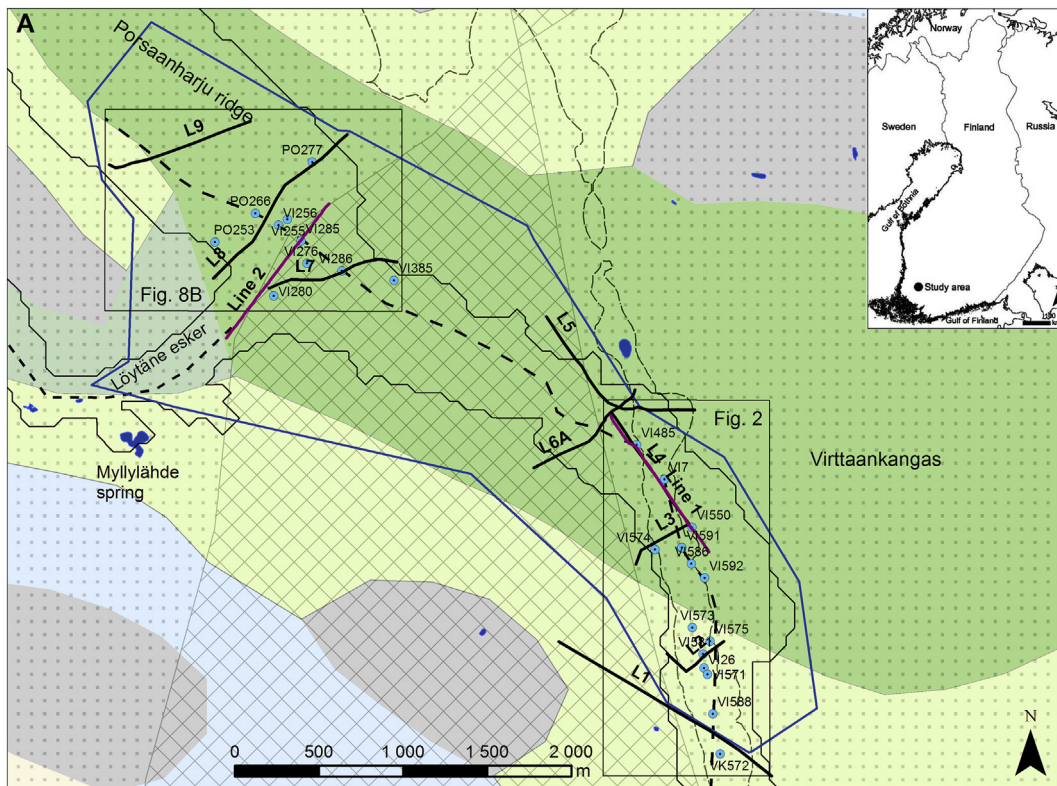
The bouldery esker core bears an arch-shaped geometry, commonly 20–40 m high and 50–150 m wide. The trend of the esker core and the Löytäne tributary esker (cf. Fig. 1a) throughout the study area has previously been based on the borehole data supplemented with a GPR-based sedimentological model. Morphologically undetectable kettle holes (MUKH) delineating the esker core were outlined by the GPR (Artimo et al., 2010). The MUKHs are in contact with the till or bedrock on their bottoms and contain large-scale deformation structures. MUKHs were formed by the subsequent collapse of sediments after the melt of buried ice blocks. The collapsed structures were later partly eroded and filled by shore processes during the regressive shoreline displacement due to the rapid glacio-isostatic land-uplift. The MUKH-structures influence the groundwater flow paths, residence times, and flow velocities, and allow the usage of reverse gradients (Artimo et al., 2010).

The Virttaankangas plain consists of six major sedimentological units: (1) Esker core, (2) subaqueous fans, (3) esker fan lobes, (4) MUKH-structures, (5) clayey bed with perched groundwater, and (6) beach deposits (Mäkinen and Räsänen, 2003). These units form the basis for the inferred units of the 3-D hydrogeological model of Virttaankangas: (a) impermeable bedrock, (b) till, (c) glaciofluvial coarse-grained sand, (d) glaciofluvial/glaciolacustrine fine-grained sand, (e) silt and clay, and (f) littoral sand (Artimo et al., 2003) (Fig. 2). The glaciofluvial coarse-grained unit (c) includes the bouldery esker core, which is the main target for the pumping wells of the MAR plant, the proximal and medial parts of the subaqueous fans, and the coarse-grained part of the ice-marginal crevasse deposits of the Porsaanharju ridge (Artimo et al., 2003). The groundwater level within the fracture valley (cf. Fig. 2) is at 86–87 m a.s.l. and about 10–23 m below the esker surface. The area covering the tributary esker core, widening of the coarse-grained hydrogeological unit, and Porsaanharju ridge has the groundwater level at 87–88 m a.s.l. and about 20–32 m below the esker surface. The tributary esker core forms a highly permeable zone that discharges part of the groundwater towards the large Myllylähde spring (ca. 2500 m<sup>3</sup>/d). The total natural groundwater yield of the Virttaankangas area is about 30,000 m<sup>3</sup>/d, whereas the MAR-plant has the current artificial recharge of about 63,000 m<sup>3</sup>/d.

## 3. Methods

The seismic lines were located on unpaved sandy and gravelly forest roads (lines L2–L7 and L9) and on paved public roads (lines L1 and L8). The seismic lines L1–L6 cover the fracture valley area, whereas lines L7–L9 focus on the area with the widening coarse-grained hydrogeological unit. The final location of the lines was selected based on varying groundwater table depths and bedrock topography as well as on the combined sedimentological and groundwater flow model. The survey compromised in total 8 km of P- and S-wave seismic lines with varying profile lengths. The data acquisition was interrupted for 5 m before and after cross-cutting water pipelines and groundwater wells to avoid infrastructure damages. The IVI vibrator MiniVibe II of COWI Denmark acted as seismic source using a 5 s linear sweep ranging from 15 to





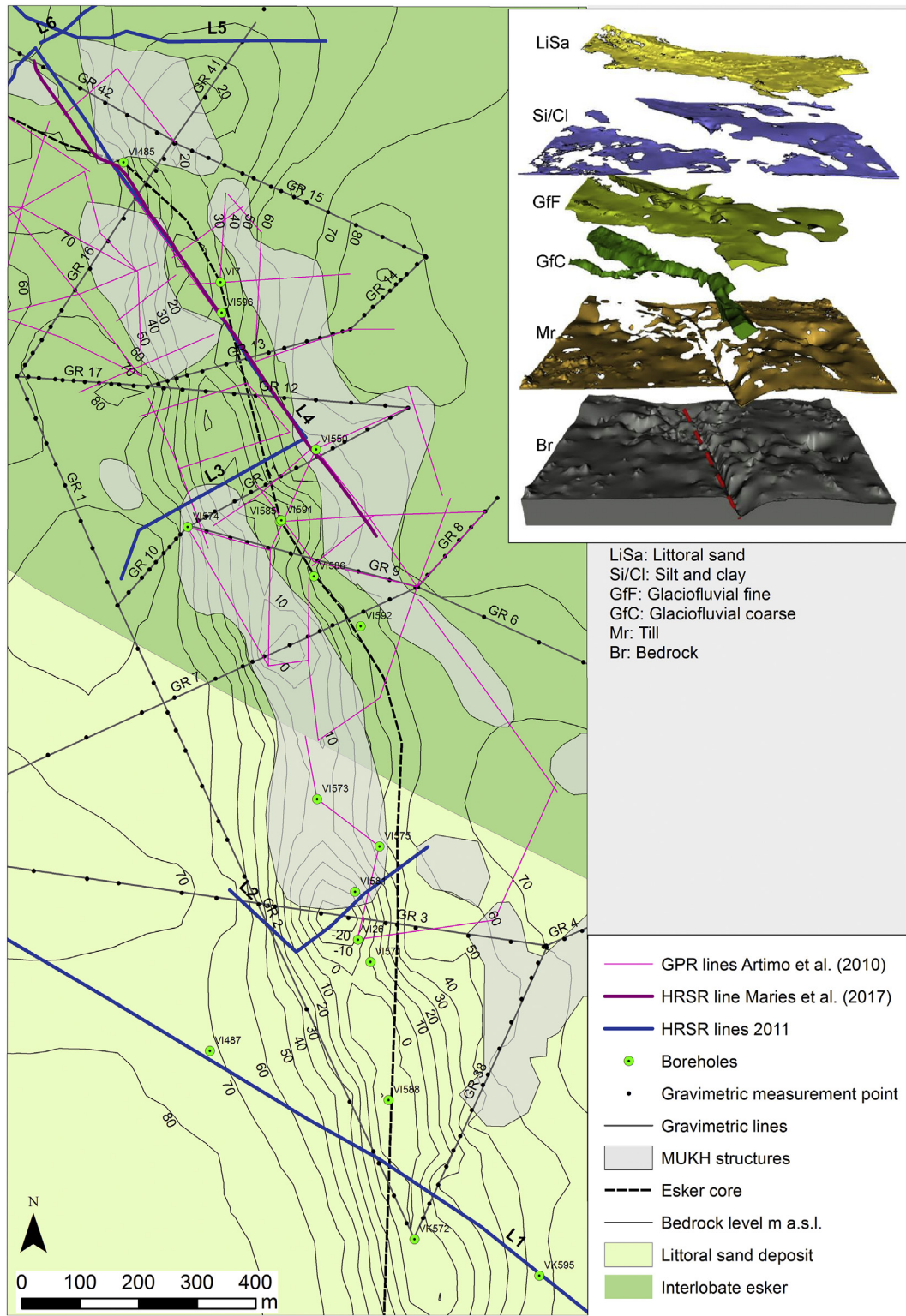


**Fig. 2.** The Virttaankangas fracture valley area with boreholes, GPR lines (Artimo et al., 2010), HRSR lines recorded in 2011 and HRSR line of Maries et al. (2017), gravimetric lines and data points, MUKH structures, trend of the esker core, and the interpolated bedrock elevation (m a.s.l.) with a 10 m contour interval (cf. Valjus, 2006). See upper right corner for the hydrogeological units of the Virttaankangas plain including the fracture valley (red dashed line) (Artimo et al., 2003, 2010).

**Fig. 1.** a) The Virttaankangas study area in SW Finland with positions of HRSR lines of 2011 and 2014 (Maries et al., 2017). National Land Survey of Finland (2016) provides the water bodies and coastline of the index figure. Turku Region Water Ltd (2016a, 2016b, 2016c) provided boreholes, MAR plant area and coarse-grained unit extent. The main esker and tributary esker cores are based on Mäkinen (2003c) and outline of the fracture valley in bedrock on Valjus (2006). Basemap and LiDAR map © National Land Survey of Finland, The modified maps of superficial deposits and bedrock of Finland © Geological Survey of Finland. b) The positions of the gravimetric lines and GPR lines of 1989 (Hänninen and Salmi, 1989) presented in the study area in addition to elements of Fig. 1a).





**Fig. 3.** a) IVI Minivib (Geological Survey of Canada). b) The 200 m landstreamer with 3-component (yellow) and vertical component geophones (red) (COWI Denmark). Photos by Elina Ahokangas, Fig. 3a taken 31.5.2011 and Fig. 3b 2.9.2011.

250 Hz (Fig. 3a). A 216-channel seismograph (Geometrics Ltd) record the earth's response for 6 s. The 200-m long landstreamer contained 48 three-component geophones with 1-m spacing and 76 vertical component geophones with 2-m spacing (Fig. 3b). The offset from the source to the first geophone station was 4 m. The seismic survey included a pre-survey test and 5 days of data acquisition in good weather conditions. A staff of 3–5 people controlled the movement of the landstreamer and good coupling of the geophones after movement. This procedure results in a cost-efficient acquisition. The altitudes for

topographic line corrections were obtained from the national airborne laser scanning data with a 2-m horizontal and 0.3-m vertical resolution.

Three new reference drillings (REF-1, REF-2, REF-4) were performed by Destia Ltd., with a 3-m bedrock confirmation after the seismic survey to support the interpretations of the seismic facies. Two of the drillings are located on line L1, where the total depth of boreholes was 10.5 m and 55.8 m. The third drilling, located on line L4, has a total depth of 78.2 m. Other boreholes in the vicinity of the seismic lines supported the data interpretation.

The seismic data was processed in three main stages (Table 1). The determination of the bedrock was based on the highest reflection energy supported by the borehole references and compared with the gravimetric data. The P-wave data (Fig. 4a) was utilized in the interpretation of the seismic facies due to its better quality compared to S-wave data (Fig. 4b). The vertical resolution of the data is ca. 5 m.

A HRSR survey (Maries et al., 2017) included 2 lines focused on the coarse-grained hydrogeological unit in order to test the applicability of the micro-electro-mechanical system (MEMS)-based landstreamer (Brodic et al., 2015) and is used for comparison. We determined five seismic facies (A-E, Table 2) in the seismic profiles integrating the data of Maries et al. (2017).

The interpretation of the seismic profiles (Figs. 5–7) is based on the synthesis of seismic facies, gravimetric data (Valjus, 2006), GPR soundings with 40 km (80 MHz antennae) (Hänninen and Salmi, 1989) and 20 km of lines (100 MHz antennae) (Artimo et al., 2010), borehole logs (Turku Region Water, 2016b), and the sedimentological model (Mäkinen, 2003c; Artimo et al., 2003). Reference boreholes were chosen according to its distance to the seismic line, which was restricted to a distance less than 50 m when possible, due to the rapid spatial changes in the esker structure and the bedrock. The accuracy of the bedrock level in the gravimetric varies between ca. 5–10 m, sometimes 10–20 m.

## 4. Results

### 4.1. The characteristics of P- and S-wave sections

The P-wave sections proved to be more useful in the characterization of the coarse-grained core and the deeper parts of the aquifer below water table and GPR range. It has markedly better penetration depth to the subsurface compared to S-wave. The P-wave sections show abundant continuous high-amplitude reflections reaching depths of 100 m from the surface (Fig. 4a). The S-wave sections show interpretable reflections only in the uppermost 20 m of the section (Fig. 4b), which is in many places above the groundwater table (dry core sediments). These sections did not provide any identifiable reflections in the main aquifer at the coarse-grained unit area or from the underlying

**Table 1**

The data processing flow for the Virttaankangas HRSR survey data (A. Pugin, Geological Survey of Canada, pers. comm. 2018).

#### 1) Processing (all data):

Format conversion, SEG2 to KGS SEGY  
1 s AGC applied for spectral whitening  
Pilot trace based deconvolution  
Separation of vertical (V), horizontal inline (H1) and horizontal crossline (H2) components  
Editing of the geometry / Sort

#### 2) P-wave – V component data:

Frequency filtering (BP 50-90-150-180 Hz)  
Scaling (trace normalization)  
Top (refractions) and airwave muting  
Velocity analysis (CMP gathers: 1 m, 2 m bins)  
NMO Correction (stacking velocities range ~500–1700 m/s)  
Stacking, maximal fold: 72  
Datum Correction for ground surface topography  
Time-depth conversion  
Export in Kingdom suite, Plot of the data

#### 3) S-wave – H1 component data:

Frequency filtering (BP 40-70-130-160 Hz)  
Scaling (trace normalization)  
Top muting (P-wave, surface waves)  
Velocity analysis (CMP gathers: 1 m bins)  
NMO Correction (stacking velocities range ~150–450 m/s)  
Stacking, maximal fold: 24  
Datum Correction for ground surface topography  
Time-depth conversion  
Export in Kingdom suite, Plot of the data

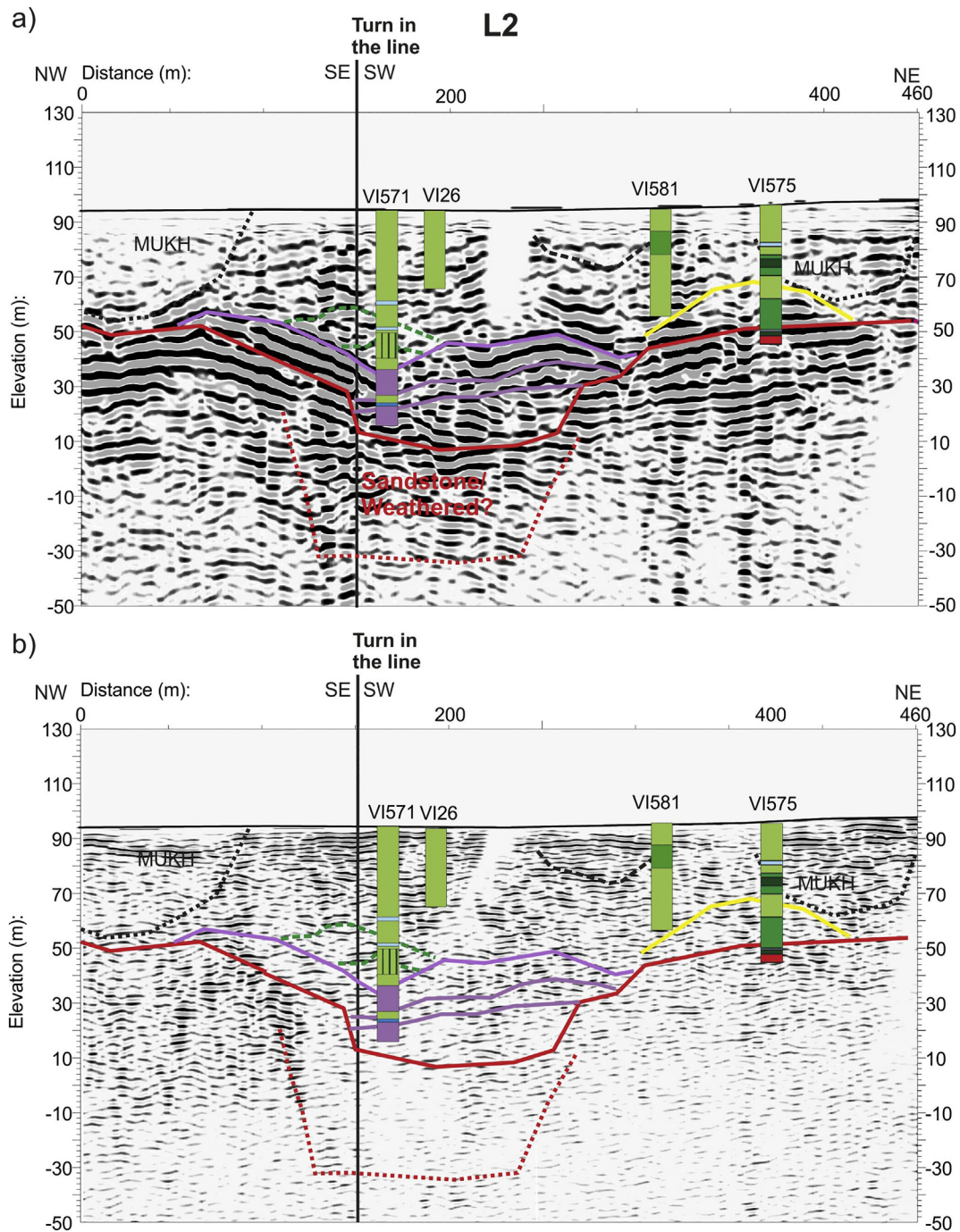


Fig. 4. a) P-wave and b) S-wave seismic profiles for the data quality comparison.

bedrock. The S-wave sections had more reflections only in the fine-grained flank area of the esker and with the presence of fine-grained sediments on the uppermost ~20 m on the esker ridge (seismic profile L5, not shown).

#### 4.2. Bedrock elevation, topography, and characteristics

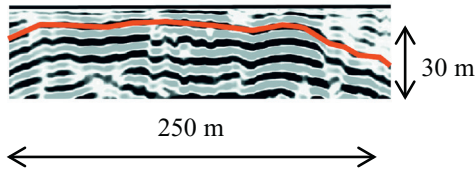
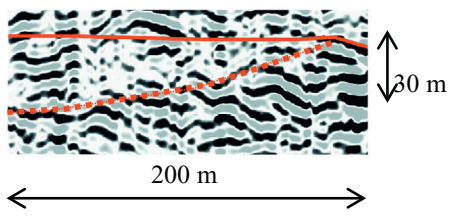
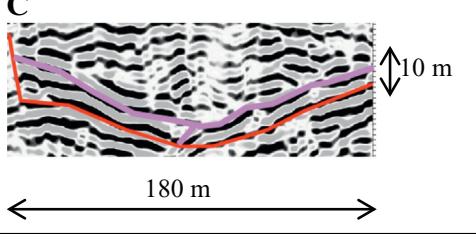
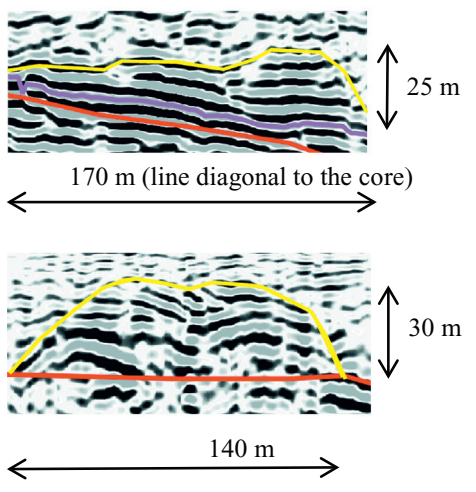
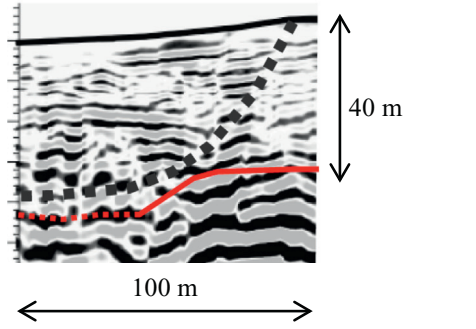
A package of continuous and strong amplitude reflections (seismic facies A) is observed on all seismic profiles (Figs. 5–7). We interpret the uppermost surface of this reflection package as the bedrock level outside the fracture valley, which is in agreement with nearby boreholes. The determination of the bedrock surface within the fracture valley is challenging, since it is overlain by 10–20 m thick diamictons that

cause high amplitude reflections. The elevation of these reflections is –10–50 m a.s.l. within the fracture valley (lines L1–L4) and 30–80 m a.s.l. outside (lines L7 and L8). This reflection package is most distinct on seismic lines L1 (distance 500–900 m and 1100–1544 m) and L2 (distance 0–150 m and 300–460 m) (Fig. 5) as well as in parts of line L4 (distance 0–300 m) (Fig. 6).

The borehole REF-1 on line L1 had 1 m of sandstone above the Svecofennian basement at 40 m a.s.l. This finding supports the assumption of a sandstone outlier beneath the Virttaankangas plain as proposed by Kaitanen and Ström (1978) and indicated by the down-ice flow Oripää esker clasts with Quartz breccia in sandstone. Boreholes VK572 (Fig. 5a), VI573 (Fig. 2) and VI592 (Fig. 2) were drilled into the fracture valley and show fracturing or weathering of the sandstone. The



**Table 2**  
The seismic facies interpretations.

Seismic facies (A-E)	Characteristics	Lithology	Sedimentological interpretation and hydrogeological implication
<p><b>A</b></p> 	<p>High amplitude reflections, mostly continuous and undulating in places.</p>	<p>Bedrock contact</p>	<p>The bedrock surface Impermeable boundary for the groundwater flow model</p>
<p><b>B</b></p> 	<p>Ascending high amplitude reflection package beneath the bedrock surface</p>	<p>Quartz diorite/ granodiorite – amphibolite/ intermediate gneiss</p>	<p>Fractured bedrock or the contact between granodiorite and mafic volcanic rocks Fracturing increases the hydraulic permeability of the bedrock</p>
<p><b>C</b></p> 	<p>High-amplitude parallel reflections overlies and follows the bedrock topography</p>	<p>Diamicton</p>	<p>Subglacial till on the bottom of the bedrock fracture (also below the esker core) Poor permeability, infills the bottom of the bedrock fracture and restricts groundwater flow to bedrock</p>
<p><b>D</b></p> 	<p>Arched geometry, horizontal (partly discontinuous) and two sets of larger convex reflections close to the bedrock (lower image).  Lower contact to a diamicton bed or bedrock surface.</p>	<p>Bouldery gravel</p>	<p>Esker core formed in a subglacial tunnel. The arched features within the core indicate boulder-rich tunnel deposits. Dimensions typical for esker cores, thickening of the core (30 m) due to overlying proximal esker fan deposits.  The hydraulically conductive esker core (main aquifer).</p>
<p><b>E</b></p> 	<p>Large concave-shaped feature with steep margins. Inner reflections chaotic and discontinuous. Lower contact to diamicton or bedrock.</p>	<p>Mixed sediments and fine-grained beds</p>	<p>MUKH structure with dislocated sediments and large-scale deformation. Influences the groundwater flow patterns and groundwater residence times (longer compared to other aquifer parts)</p>

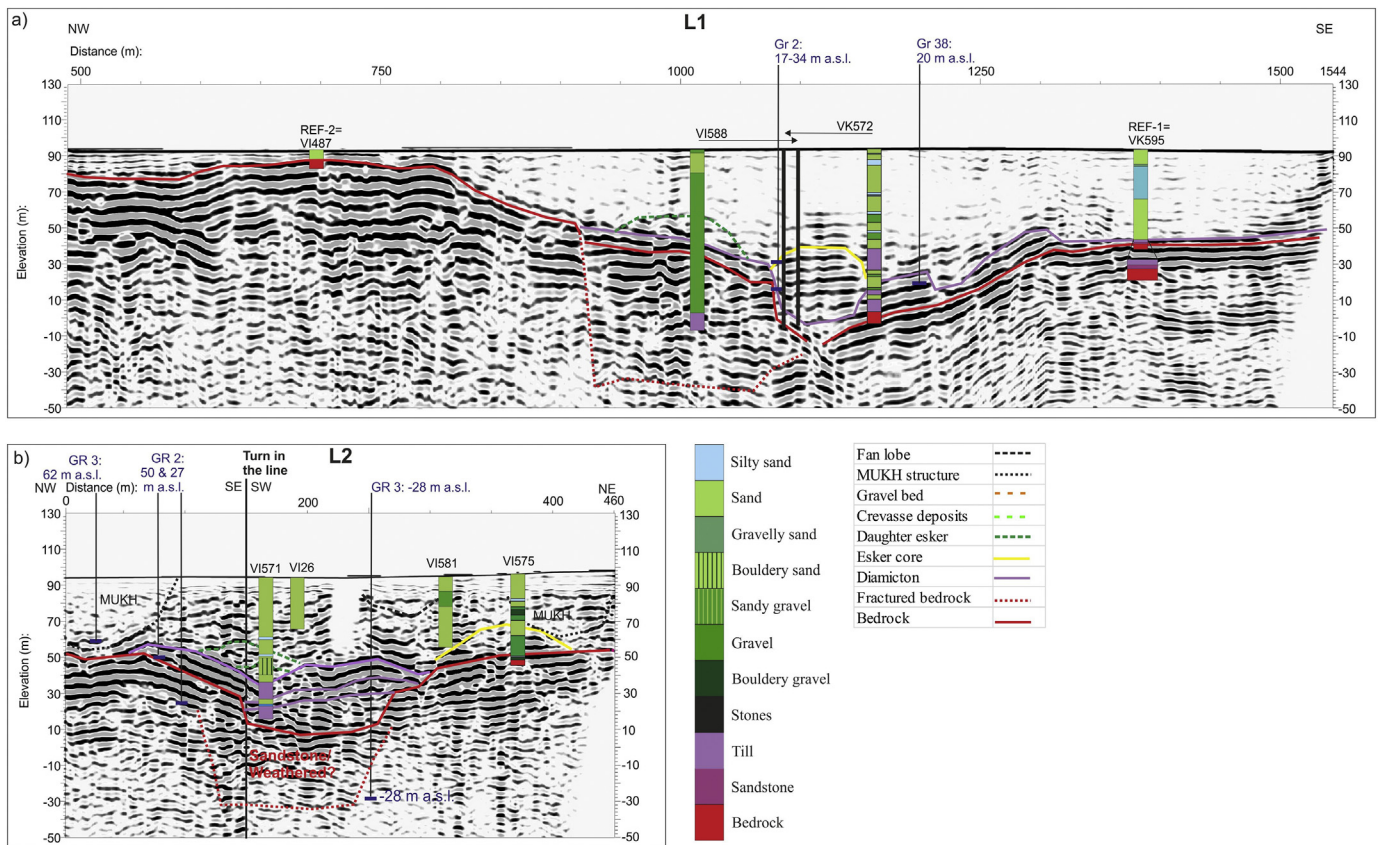


**Fig. 5.** The interpreted seismic profiles a) L1 and b) L2 in the southern part of the fracture valley with borehole logs (max. 50 m distance from the seismic profile) and bedrock elevations (m a.s.l.) based on the gravimetric data. Borehole projection along the assumed esker core direction is indicated (black arrows).

fracturing increases the amount of high amplitude reflections in the bedrock reflection package. The distinctness of the bedrock reflection package on line L7 (seismic facies B, Table 2) is related to the changes in the rock composition from quartz diorite/granodiorite to amphibolite and intermediate gneiss (Salli, 1953a, 1953b) (cf. Fig. 1). The strong horizontal reflections beneath the arched reflection package indicate fracturing of the bedrock on line L7 (Fig. 7). Borehole VI280 at the WSW end of line L7 revealed fracturing in the bedrock. These observations support the fracturing of the bedrock in places on the Porsaanhjarju main ridge area. An ascending reflection (20–50 m a.s.l.) (seismic facies B, Table 2) detected below the interpreted bedrock level at a distance of 200–650 m to line L8 (Fig. 7b) could either be related to a change in the bedrock lithology or to a fractured zone within the bedrock.

### 4.3. Seismic and sedimentary stratigraphy

#### 4.3.1. The diamictons

Strong reflection packages following the interpreted underlying bedrock topography (seismic facies C, Table 2) fill the deepest parts of the fracture valley (lines L1–L4) (Figs. 5, 6). These reflections are discontinuous in some places, especially at a distance of 1050–1250 m to line L1 and at a distance of 100–200 m line L2 (Fig. 5). Based on the borehole data, the strong reflection packages within the fracture valley are composed of diamictons below the esker core. The 101 m deep borehole VI588 (Fig. 5) reveals a 10-m thick diamicton at the bottom (–7 m a. s.l.). The projection of VI588 along the esker core fits well with the interpreted seismic facies on seismic line L1 (Fig. 5a). Three separate reflection packages (5–20 m thick) are found on top of the bedrock on seismic line L2 (Fig. 5b). The adjacent borehole VI571 shows two diamicton units (partly with angular stones) about 7.5 m thick separated by a 4 m thick fine-grained sandy layer with clay fragments that

matches relatively well with the reflection patterns. Two diamicton beds separated by 10 m thick sandy and gravelly beds (Fig. 5a) are also found in borehole VK572 outside the esker core south of line L1.

#### 4.3.2. The esker core (main aquifer)

All seismic lines (L1–L9) revealed distinct arch-shaped seismic facies D with slightly varying appearances (cf. Table 2). Boreholes verify this interpretation by coarse-grained material (gravel/bouldery gravel/boulders). We interpret this seismic facies as the esker core (cf. Pugin et al., 2009a; Oldenborger et al., 2013; Burschil et al., 2018). The seismic facies D overlying the bedrock was most distinct on seismic line L8. On line L7, the reflections of the core are weaker and identified based on the boulder-rich gravel in borehole VI286. The seismic data indicates that the core is 20–35 m high and 80–160 m wide, corresponding well with the existing depositional model. The two arc-shaped features (width 30–50 m and height 12–20 m) inside the esker core and above the diamicton on seismic lines L2 (Fig. 5b) and L3 (Fig. 6a) might indicate boulder-rich tunnel deposits. The esker core was detected on top of the diamicton beds in seismic lines L1–L4 (Figs. 5, 6). On lines L1 and L3, the arch-shaped package lays in the deepest part of the fracture valley. On lines L1 and L2, two separate esker cores are present on the western flank of the fracture valley (Fig. 5). The additional core in seismic lines L1–L2 is interpreted to present a daughter esker (Hooke, 2005) i.e. a secondary core diverging from the main esker (cf. Mäkinen, 2003c). This interpretation is supported by a tracer test of groundwater investigations (Artimo et al., 2010).

Two esker cores are detected on seismic line L4 and one esker core is located on line L8. They consist of thicker ramps that usually correspond to the proximal fan environments (Mäkinen, 2003a). The wide and complex reflection patterns to the west of the main core on seismic line L7 are interpreted as the gravelly tributary esker deposits.



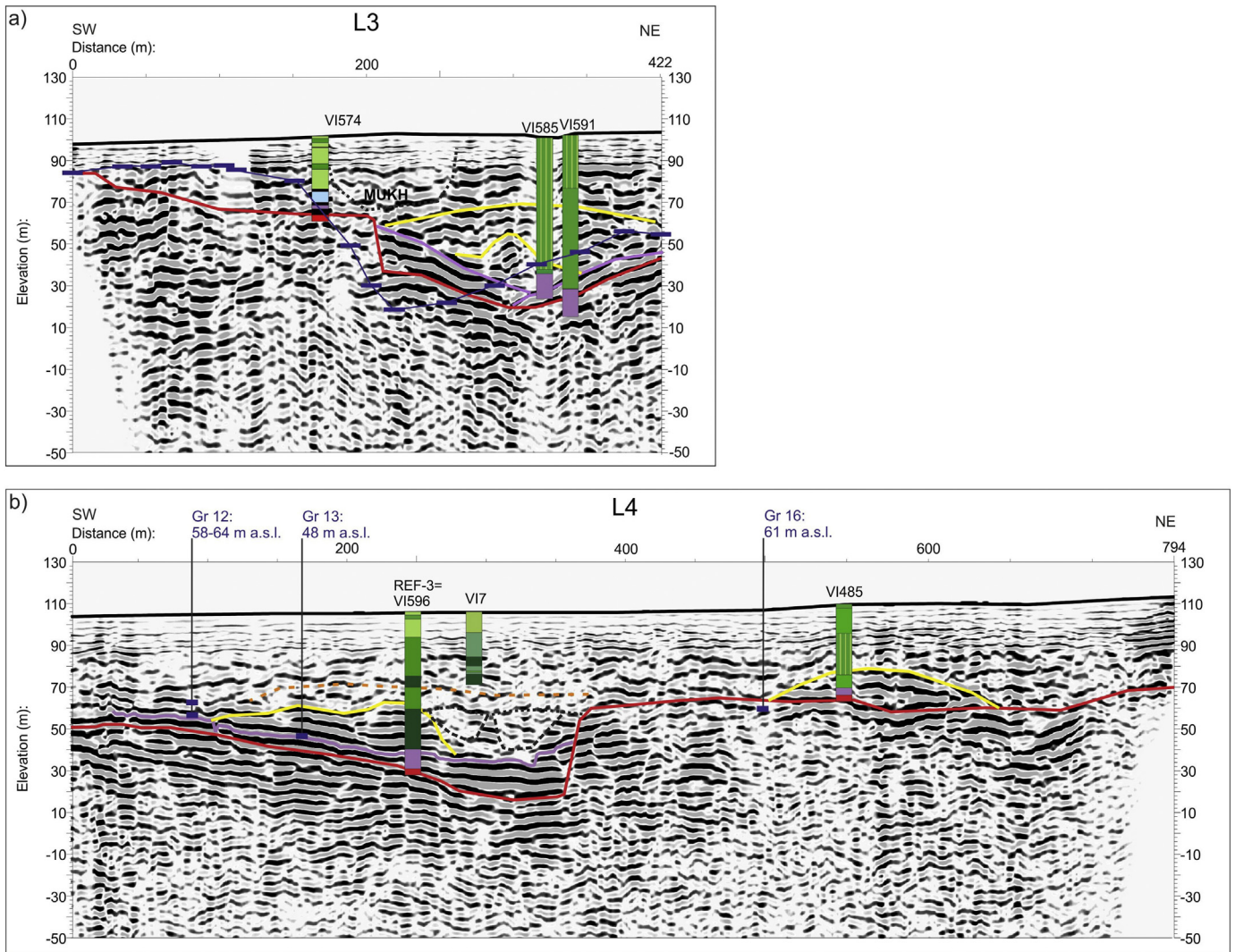


**Fig. 6.** a) The interpreted seismic profile L3 with bedrock level comparison based on the gravimetric measurement points of gravimetric lines GR 10 and GR 11 (35–50 m) distance from L3). b) The seismic line L4 in the northern part of the fracture valley with borehole logs (max. 50 m distance from the seismic line) and bedrock elevations (m a.s.l.) based on the gravimetric measurement point data.

Moreover, our interpretation of line L7 to shows the coalescence of the tributary and the main core (Fig. 7a), which is likely related to a large bouldery esker fan about 400 m southeast (Mäkinen, 2003c). A secondary arch-shaped feature was identified on seismic line L8 (7–20 m thick, 200 m wide) adjacent to borehole PO277 (Fig. 7b) and on line L9 (not shown). It is interpreted as the crevasse deposits associated with the marked enlargement of the glaciofluvial complex on the NE side of the repeated esker fans (Mäkinen, 2003c).

#### 4.3.3. Esker fans

Two large trough-shaped features with a continuous overlaying horizontal bed (cf. Maries et al., 2017), consisting of bouldery gravel (borehole VI596), are found next to the esker core on line L4 (Fig. 6). Their inner reflections are weaker compared to the surroundings. The troughs are interpreted as esker fan lobe channels deposited within a restricted fracture valley and the horizontal bed as part of the esker fan sediments, based on the observations of Maries et al. (2017). However, we did not recognize the fan lobes elsewhere. The sediments overlapping the esker core are related to repeated and overlapping subaqueous fans with large cross-bedded fan lobes identified by the GPR near the surface at the

Virttaankangas area (Mäkinen, 2003c; Artimo et al., 2010; Maries et al., 2017).

#### 4.3.4. MUKH structures

Large trough-shaped structures (seismic facies E, Table 2) with abrupt margins and changed or bended seismic reflections were detected on the upper and middle parts of seismic lines L2 (Fig. 5b), L3 (Fig. 6a) and L8 (Fig. 7b). Their inner reflection pattern appears chaotic with discontinuous reflectors. These trough-shaped features are often in close contact with diamicton or the bedrock. We interpret these as MUKH structures, which have previously been found in the Virttaankangas area, based on GPR surveys (Mäkinen, 2003c; Artimo et al., 2010). Two MUKH structures are present at both ends of the seismic line L2, flanking the esker core sediments (Fig. 5b). A large MUKH structure can be identified at the WSW end of seismic line L7, the bedrock contact of which has been confirmed by the higher resolution seismic survey by Maries et al. (2017). In addition, seismic line L8 shows the eastern margin of a large MUKH complex detected in earlier GPR soundings (Mäkinen, 2003c) (Fig. 8a). This MUKH structure is located between the main esker core and its secondary branch feeding the wide

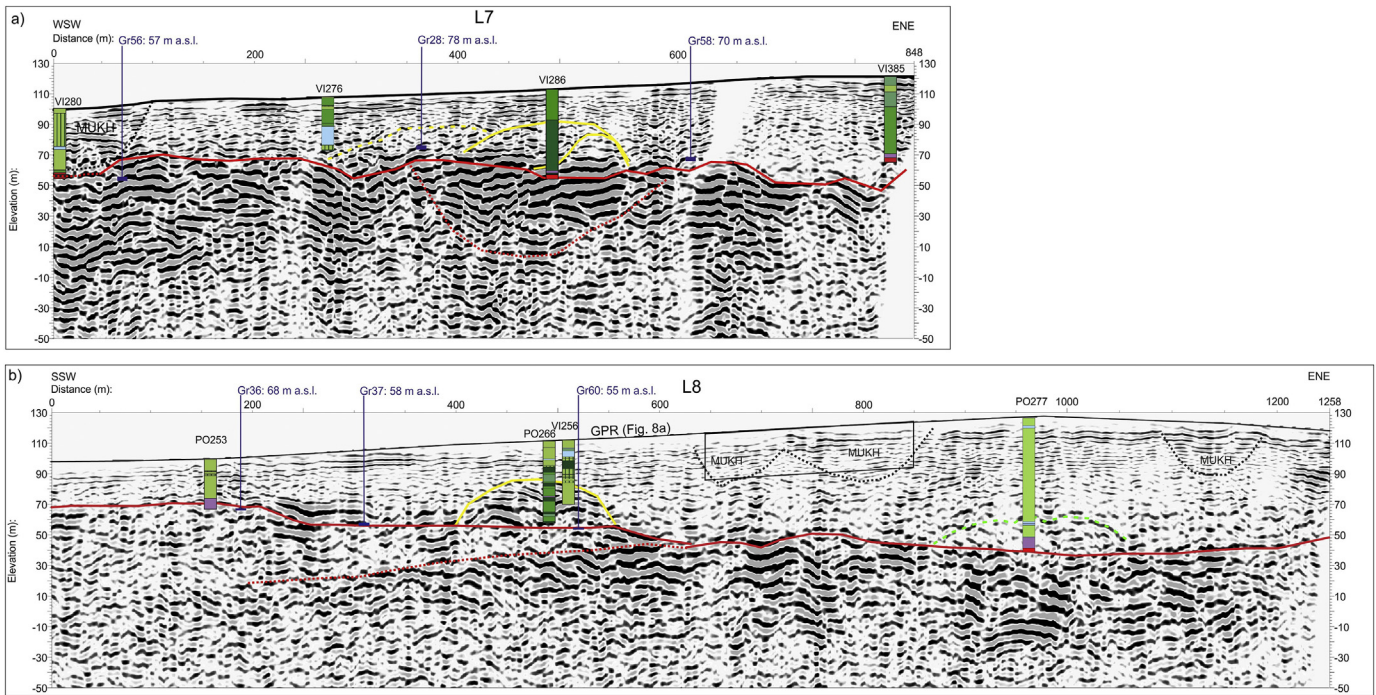


**Fig. 7.** The interpreted seismic profiles a) L7 and b) L8 adjacent to the widening of the coarse-grained unit with borehole logs (max. 50 m distance from the seismic profile) and bedrock elevations (m a.s.l.) based on the gravimetric data.

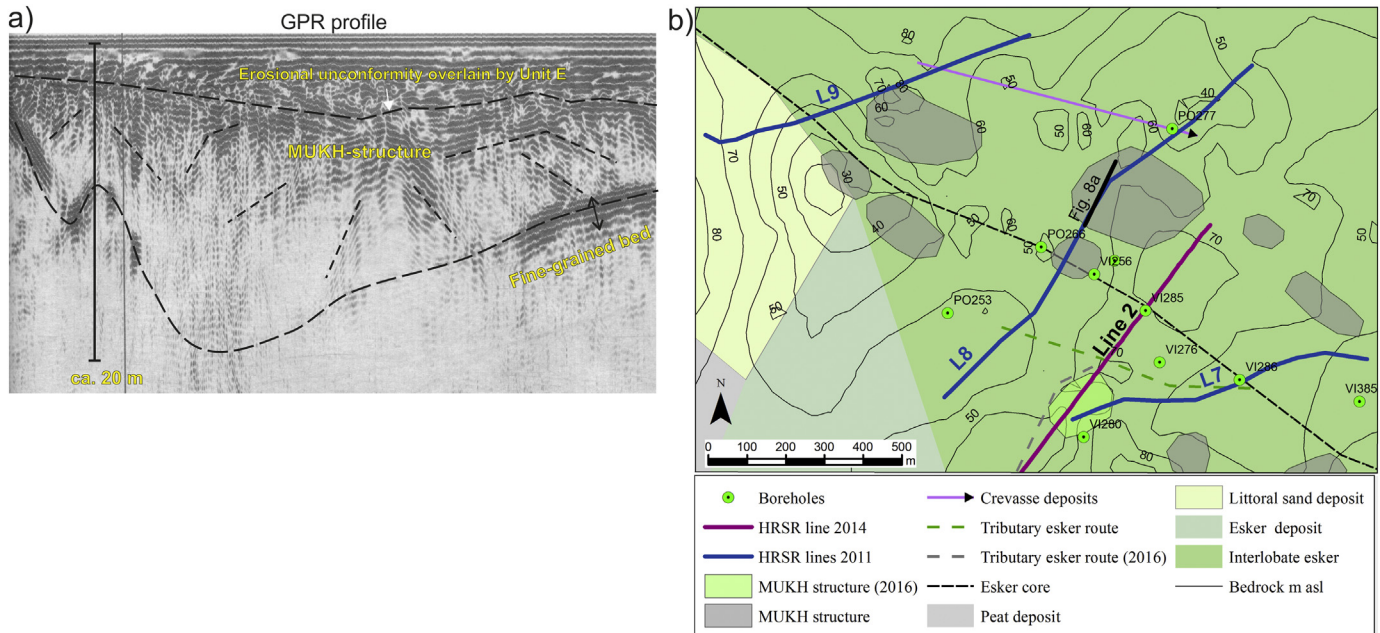


**Fig. 8.** a) GPR section with interpreted MUKH structure (Mäkinen, 2003c) parallel to seismic line L8. b) The interpreted new tributary esker route joining the main esker at line L7 and crevasse deposits near the widening of the coarse-grained unit on lines L8 and L9 shown with the boreholes, MUKHs, (main) esker core and bedrock topography.

glaciofluvial enlargement on the northeastern side of the esker fans (Fig. 8b).

## 5. Discussion

### 5.1. The impact of the geological conditions on the HRSR survey

The HRSR survey was carried out on thick and heterogeneous Virttaankangas interlobate esker sediments lacking overlapping fine-

grained beds or till beds that are common in tunnel valley environments in North Europe and Canada (Huuse et al., 2003; Kirsch et al., 2006; Ahmad et al., 2009; Oldenborger et al., 2013, 2016). The P-waves had to propagate through thick and complex sediment units prior to reaching the groundwater level in depth of 10–30 m. This resulted in poorer signal-to-noise ratio due to large energy loss in the unsaturated zone. The characteristics of the heterogeneous sediments also vary rapidly which leads to rapid velocity variations in them. The transition from unsaturated to saturated zone causes more complications as it is



common for the P-wave velocity in unconsolidated sediments to increase by a factor of four or more at the transition from dry or partial water saturation to full saturation (Bradford and Sawyer, 2002).

The interpretation of P-wave reflections as seismic packages, surfaces, and facies (Mitchum et al., 1977) was applied in this work within the limits of the data resolution. The quality of the P-wave data compared to S-wave data was significantly better (cf. Fig. 4), unlike other HRSR surveys (Pugin et al., 2004, 2009a). The P-wave reflections with higher amplitudes were more identifiable within the coarse-grained unit and the deeper parts of the aquifer. The S-wave data suffered from attenuation due to the abundant coarse-grained esker sediments (gravels) (cf. Pugin et al., 2006, 2009a) and provided high-amplitude reflections mostly in the uppermost 20 m. Therefore, we did not utilize them in the characterization of the deep parts of the aquifer.

GPR shows advances compared to seismic investigations in the interpretation of the topmost 20–25 m and in the construction of the depositional model and related depositional stages. The 5-m resolution of the seismic survey constrained the amount of identifiable sedimentary structures in P- and S-wave profiles. The P-wave profiles showed only some of the major sedimentary structures like the MUKHs and through-shaped fan lobes (Figs. 5, 6). The S-wave profiles provided more reflections compared to P-waves in the uppermost 20 m of deposits but could not provide as detailed imaging of the sedimentary structures as the GPR profiles (80 and 100 MHz antennae). The S-wave profiles did not provide additional value to the definition of the hydrogeological units. The GPR lines (Hänninen and Salmi, 1989; Artimo et al., 2010) allowed the definition of the hydrogeological units. They were highlighted in the accurate identification and positioning of the MUKH structures and in characterization of the esker fans or lobes.

In general, considering the 5-m vertical resolution, it was very difficult to define the sedimentary structures of the esker fan deposits from the seismic reflections reliably. The interpretation of the esker stratigraphy and bedrock elevation within the fracture valley was challenging due to various bedrock conditions, the presence of sandstone and overlying diamictons. The seismic resolution is also the reason that we only recognize the esker fan lobes on line L4. The synthesis of all data sets (boreholes, GPR, and gravimetry lines), existing sedimentological and hydrogeological models, projection of the boreholes according to the trend of the esker core and the fracture valley, together with the information from the higher resolution seismic landstreamer survey (Maries et al., 2017) improved the interpretation of the seismic data.

The interpretation of the reflections along each seismic line is also influenced by the distance of the available boreholes to the line. When boreholes are found <50 m distance from the seismic lines, they provide more reliable reference of the lithology variations, since large variations can occur within few tens of meters in the interlobate esker environment due to high heterogeneity of sediments and varying thickness of the dry core (cf. Mäkinen, 2004). This is further reflected to the accuracy of the velocity analysis.

## 5.2. The characterization of the bedrock and diamicton

The bedrock elevation provided by the gravimetric data is in general in good agreement with the interpreted seismic bedrock level outside the fracture valley. The bedrock elevation varies in the order of 5–10 m. Inside the fracture valley, gravimetrically determined bedrock elevation does not correspond well with the interpreted seismic data bedrock elevation (for comparison see L3, Fig. 6a). The gravimetric data could not distinguish between the compact diamicton beds resting on top of the bedrock and the bedrock. This resulted in a false bedrock level (10 m) as shown by the drilling REF-3 compared to the gravimetric line (line GR 13) on seismic line L4 (Fig. 6b). The bedrock level

interpretation from gravimetric data is in better agreement with seismic data where there is no thick diamicton present (L4: GR 16). The combined effect of the coarse-grained esker core, diamicton beds, and fractured bedrock may cause accuracy variations to the gravimetric data. Their relatively high densities can distort the bedrock level interpretation. The impedance contrast between Quaternary sediments and weathered bedrock with solid bedrock is usually very strong (cf. Pugin et al., 2006) but seems to be lacking in the fracture valley at Virttaankangas. This further complicated the separation of bedrock (solid and weathered), diamicton, and esker core signals.

Fracturing of the steep flank of the fracture valley on line L4 (Fig. 6b) was not detected in this survey in contrast to the survey of Maries et al. (2017). Some high amplitude bedrock reflections are related to the variously fractured bedrock and might be enhanced where they occur straight below the esker core in seismic line L7 (Fig. 7a). They are similar to those described by Maries et al. (2017) from the seismic line only 300 m to the northwest. It is possible that pressurized water in the subglacial tunnel was forced into the fractured bedrock leading to further fracturing (cf. Boulton et al., 2007, 2009). The distinctness of bedrock reflections on seismic line L7 and the dipping reflection within the bedrock point to a bedrock contact between granodiorite and quartz diorite and mafic volcanic rocks.

The presence of sandstone on seismic line L1, assumed as a possible outlier of the Satakunta sandstone (Kaitanen and Ström, 1978), is supported by the lower velocities at the bottom of the fracture valley (3000 m/s, Maries et al., 2017). This velocity is lower than the seismic velocity of the bedrock in the Porsaanharju-Virttaankangas area outside the major fracture valley, determined to be >5000 m/s at the ends of profile 1 by Maries et al. (2017) and in the range of 4300–5100 m/s by a refraction survey (Maa ja Vesi Ltd., 1975).

The low seismic velocity contrasts of sandstone, fractured bedrock, diamicton beds, and esker core sediments as well as the limited resolution hampers the separation of these units. This can also be observed in the Suupohja region in Western Finland, ca. 120 km north from the study area, where disintegrated (weathered) bedrock or sandstone occurs below Quaternary sediments (Pitkäranta, 2013).

## 5.3. The characterization of the main aquifer (esker core) and esker elements

The main aquifer, i.e. the esker core, can be well depicted from the seismic data, even without the borehole reference. It shows an arched geometry and high amplitude, continuous horizontal to partly discontinuous convex reflections. The arch-shaped reflection of the esker core within the fracture valley depicted in Maries et al. (2017) was not as distinct as in our study, for the material and the reflections of the esker core and the surrounding coarse-grained proximal fan deposits were quite similar. The interpretation of the esker core trend and core dimensions from the seismic data matches well with those predicted by the existing depositional model used for the groundwater flow model (Artimo et al., 2003, 2010). However, our results reveal a daughter esker west of the main esker core within the middle part of the fracture valley. This is also indicated by the results of the groundwater investigations in Virttaankangas (Artimo et al., 2010). The presence of the coarse-grained sediments of the two esker cores explains the exceptionally good pumping well yield in the southern part of the fracture valley.

The seismic data confirms the widening of the coarse-grained hydrogeological unit at the NW end of the area. It shows the coalescence of the main and the tributary cores (Fig. 8b) with their widespread highly permeable gravels. This explains short residence times, of flow path simulations of the groundwater flow model, in relation to the recharge from the infiltration ponds adjacent to seismic line L7.

Furthermore, the high-amplitude reflections from the bedrock just below the esker core in seismic line L7 have similar reflection patterns to those described on line 2 of Maries et al. (2017) (cf. Fig. 1). Line 1 of Maries et al. (2017) parallel to line L4 shows the same positions for the esker core both outside and inside fracture valley. The poor hydraulic permeability of the diamictons significantly influences the groundwater interaction between the aquifer and the underlying fractured bedrock in the fracture valley (cf. Maries et al., 2017).

The resolution of this survey did not allow the identification of more detailed seismic facies related to the esker fans or lobes. The identification of the fan lobes within the fracture valley (seismic line L4) was due to the velocity contrast between the more finer-grained fan lobes and the surrounding bouldery gravel sediments. The distinction and details of MUKH structures were weaker compared to data of Maries et al. (2017) where faulting in the sediments of the MUKH structures was detected as well. However, the MUKHs in the seismic lines of this survey were in agreement with the GPR-based MUKH positions (Mäkinen, 2003c; Artimo et al., 2010).

The coarse-grained sediments encountered in this survey with lower velocity contrast between units make the identification of different seismic facies more difficult. In comparison, buried valley aquifers with overlying and saturated fine-grained tills and marine sediments show clear velocity contrasts to the glaciofluvial esker deposits (Pugin et al., 2009a). In Virttaankangas, till deposits are found only on top of the bedrock, in places eroded by the meltwater processed preceding esker deposition (cf. Maries et al., 2017) and overlain by the esker core. The Säkyänharju-Virttaankangas esker sediments also filled the fracture valley completely, while in the North American and North European tunnel valleys, eskers run along the bottoms of tunnel valleys of different sizes and with other types of infilling sediments, often with multiple till beds within or on top of the deposits (cf. Ahmad et al., 2009; Pugin et al., 2014).

## 6. Conclusions

This first high-resolution seismic-reflection landstreamer survey in thick and complex interlobate esker deposits in Finland proves the applicability of the method for aquifer characterization and stratigraphic studies in thick Quaternary sediments. The method is highly applicable to sediments in glaciated areas and glaciofluvial deposits of lesser thickness and especially with aquifers covered with fine-grained sediments that are not accessible by ground penetrating radar. If there are usable roads or paths for the landstreamer, the survey allows fast and cost-effective seismic data acquisition and guides the position of well-targeted boreholes, which strengthen the interpretation of depositional and hydrogeological units especially in stratigraphically complex settings. The higher penetration depth of the HRSR method (over 100 m) over the GPR (20–25 m) favors its use in the study of thick esker sediments. The P-wave sections showed the seismic facies in the deeper parts of the aquifer while the S-wave sections revealed details only in the uppermost 20 m. The GPR surveys are needed in the case of shallow sedimentological modeling when the resolution of the HRSR survey remains in 4–5 m and inhibits the identification of more detailed sedimentary structures. We identify several seismic facies from both the bedrock (bedrock surface and contact, fractured bedrock) and the sediments (diamicton beds, esker core, and MUKH structures).

The detection of the bedrock surface elevation and its topographic variations was achieved with good accuracy on all profiles supported by reference boreholes. In places, fracturing and lithological changes in the bedrock were also detected, adding to the value of HRSR landstreamer data. However, the separation of fractured and weathered bedrock from overlying diamicton beds and boulder-rich esker core posed a challenge due to similarities in seismic facies within the fracture

valley. The use of reference boreholes can help to overcome these problems.

The HRSR data support the earlier classification of the large-scale hydrogeological units that form the basis for the groundwater flow model of the Virttaankangas MAR plant. The position and the geometry of the main aquifer with the esker core and the seismic facies variability were detected with good accuracy in all seismic profiles, revealing detailed information of the coarse-grained unit and confirming the hydrogeological model. Two previously unknown features of the esker core in two different parts of the aquifer were revealed: (1) The presence of a daughter esker adjacent to the main esker core that explains the good hydraulic conductivities in the southern part of the Virttaankangas fracture valley and (2) the widening of the coarse-grained hydrogeological unit in association with the tributary esker core and the secondary ice-marginal branch of the main core. Moreover, MUKH structures influencing the groundwater flow and flow velocity were also depicted by HRSR. These new findings of the coarse-grained unit are of high importance for the 3-D hydrogeological model, allowing more comprehensive understanding of the groundwater flow conditions and, therefore, improving the hydrogeological model.

## Declaration of Competing Interest

The authors declare that they have no known competing financial interests or personal relationships that could have appeared to influence the work reported in this paper.

## Acknowledgements

The original data presented in this paper are available upon request from the corresponding author. This research was funded by the K.H. Renlund Foundation, Finnish Water Utilities Association (FIWA) and Turku Region Water Ltd. Elina Ahokangas was funded by the grants awarded by the Alfred Kordelin Foundation and Finnish Cultural Foundation Central Fund. We are grateful to Tracy Brennand, Hazen Russell and Jörg Lang as well as the two anonymous reviewers for their constructive comments. We thank André Pugin (Geological Survey of Canada) in particular for the processing of the seismic data and Søren Wedel Nielsen (COWI Denmark) for fluent collaboration during data acquisition. Professional traffic control during the field work on public roads was provided by the Military Police from the Säkyälä Army Base and the traffic signs by Destia. Additional support for the landstreamer operation was given by Pekka Huhta, Risto Kiuru, Kati Suhonen and Juha Mursu from the Geological Survey of Finland. Osmo Puurunen and Sami Saraperä from the Turku Region Water Ltd. provided help with field-work arrangements.

## References

- Maa ja Vesi Oy, 1975. Säkyänharjun-Virttaankangas pohjavesiselvitys. (The groundwater investigation of Säkyänharju-Virttaankangas). 17 p. Report 1975-08-22. Available from: Turku Region Water Ltd, Maariankatu 1, FI-20100 Turku, Finland (In Finnish).
- Ahmad, J., Schmitt, D.R., Rokosh, C.D., Pawlowicz, J.G., 2009. High-resolution seismic and resistivity profiling of a buried Quaternary subglacial valley: Northern Alberta, Canada. *Geol. Soc. Am. Bull.* 121, 1570–1583. <https://doi.org/10.1130/B26305.1>.
- Ahokangas, E., Mäkinen, J., 2014. Sedimentology of an ice-margin esker with implications for the deglacial dynamics of the Finnish Lake District lobe trunk. *Boreas* 43, 90–116. <https://doi.org/10.1111/bor.12023>.
- Artimo, A., Mäkinen, J., Berg, R.C., Abert, C.C., Salonen, V.-P., 2003. Three-dimensional geologic modeling and visualization of the Virttaankangas aquifer, southwestern Finland. *Hydrogeol. J.* 11, 378–386. <https://doi.org/10.1007/s10040-003-0256-6>.
- Artimo, A., Saraperä, S., Ylander, I., 2008. Methods for integrating an extensive geodatabase with 3D modeling and data management tools for the Virttaankangas artificial recharge project, southwestern Finland. *Water Resour. Manag.* 22, 1723–1739. <https://doi.org/10.1007/s11269-008-9250-z>.
- Artimo, A., Saraperä, S., Puurunen, O., Mäkinen, J., 2010. The Turku Region Artificial Infiltration Project, Finland – tools for enhanced aquifer characterization. *The 7<sup>th</sup> Annual*



- International Symposium on Managed Aquifer Recharge (ISMAR). Abu Dhabi, October 9–13, 2010.
- Barnett, P.J., Sharpe, D.R., Russell, H.A.J., Brennard, T.A., Gorrell, G., Kenny, F.M., Pugin, A.J.-M., 1998. On the origin of the Oak Ridges Moraine. *Can. J. Earth Sci.* 35, 1152–1167. <https://doi.org/10.1139/cjes-35-10-1152>.
- Boulton, G.S., Lunn, R., Vidstrand, P., Zatzepin, S., 2007. Subglacial drainage by groundwater-channel coupling, and the origin of esker systems: part II—theory and simulation of a modern system. *Quat. Sci. Rev.* 26, 1091–1105. <https://doi.org/10.1016/j.quascirev.2007.01.006>.
- Boulton, G.S., Maillot, P.B., Zatzepin, S., 2009. Drainage beneath ice sheets: groundwater-channel coupling, and the origin of esker systems from former ice sheets. *Quat. Sci. Rev.* 28, 621–638. <https://doi.org/10.1016/j.quascirev.2008.05.009>.
- Bradford, J.H., Sawyer, D.S., 2002. Depth characterization of shallow aquifers with seismic reflection, Part II—Prestack depth migration and field examples. *Geophysics* 67, 98–109. <https://doi.org/10.1190/1.1451372>.
- Brennard, T., Shaw, J., 1996. The Harricana complex, Abitibi region, Quebec: their implications for ice-sheet meltwater regime and ice sheet dynamics. *Sedim. Geol.* 102, 221–262. [https://doi.org/10.1016/0037-0738\(95\)00069-0](https://doi.org/10.1016/0037-0738(95)00069-0).
- Brodic, B., Malehmir, A., Juhlin, C., Dynesius, L., Bastani, M., Palm, H., 2015. Multicomponent broadband digital-based seismic landstreamer for near-surface applications. *J. Appl. Geophys.* 123, 227–241. <https://doi.org/10.1016/j.jappgeo.2015.10.009>.
- Brodic, B., Malehmir, A., Pugin, A.J.-M., Maries, G., 2018. Three-component seismic land streamer study of an esker architecture through S- and surface-wave imaging. *Geophysics* 83, 1–16. <https://doi.org/10.1190/geo2017-0747.1>.
- Burke, M.J., Woodward, A.J., Russell, A.J., Fleisher, P.J., Bailey, P.K., 2008. Controls on the sedimentary architecture of a single event glacial esker: Skeidararjökull, Iceland. *Quat. Sci. Rev.* 27, 1829–1847. <https://doi.org/10.1016/j.quascirev.2008.06.012>.
- Burschil, T., Buness, H., Tanner, D.C., Wielandt-Schuster, U., Ellwanger, D., Gabriel, G., 2018. High-resolution reflection seismic records reveal the structure and the evolution of the Quaternary glacial Tannwald Basin. *Near S. Geophys.* 16, 593–610. <https://doi.org/10.1002/nsg.12011>.
- Cummings, D.I., Russell, H.A.J., 2007. The Vars-Winchester Esker Aquifer, South Nation River Watershed, Ontario. CANQUA Field Trip, June 6<sup>th</sup> 2007, Geological Survey of Canada, Open File 5624 (74 p).
- Cummings, D.I., Gorrell, G., Guilbaut, J.P., Hunter, J.A., Logan, C., Ponomarenko, D., Pugin, A.J.-M., Pullan, S.E., Russell, A.J., Sharpe, D.R., 2011. Sequence stratigraphy of a glaciated till basin fill, with a focus on esker sedimentation. *Geol. Soc. Am. Bull.* 127, 1478–1496. <https://doi.org/10.1130/B30273.1>.
- Gruszka, B., Morawski, W., Zieliński, T., 2012. Sedimentary record of a Pleistocene ice-sheet inter-lobate zone (NE Poland). *Geologos* 18, 65–81. <https://doi.org/10.2478/v10118-012-0005-1>.
- Hämäläinen, A., 1994. Geological map of Finland. Pre-Quaternary rocks. Sheet 1134 Kokemäki. Geological Survey of Finland, Espoo.
- Hänninen, P., Salmi, M., 1989. Maatutkaluotaus Virttaankankaalla. (Ground penetrating radar survey at Virttaankangas) 5 p. Geological Survey of Finland Research Explanation P32.4.002.
- Hooke, R. LeB., 2005. *Principles of Glacier Mechanics*. 429 pp. Cambridge University Press, Cambridge.
- Huuse, M., Piotrowski, J.A., Lykke-Andersen, H., 2003. Geophysical investigations of buried Quaternary valleys in the formerly glaciated NW European lowland: significance for groundwater exploration. *J. Appl. Geophys.* 53, 153–157. [https://doi.org/10.1016/S0926-9851\(03\)00115-0](https://doi.org/10.1016/S0926-9851(03)00115-0).
- Inazaki, T., 2004. High-resolution seismic reflection surveying at paved areas using an S-wave type Land Streamer. *Explr. Geophys.* 35, 1–16. <https://doi.org/10.1071/EG04001>.
- Kaitanen, V., Ström, O., 1978. Shape development of sandstone cobbles associated with the Säkyliä-Mellilä esker, SW Finland. *Fennia* 155, 23–66.
- Kirsch, R., Rumpel, H.M., Scheer, W., Wiederhold, H., 2006. *Groundwater Resources in Buried Valleys – A Challenge for Geosciences*. Leibniz Institute for Applied Geosciences (GGA-Institut), Hannover, Germany 303 p.
- Krawczyk, C.M., Polom, U., Trabs, S., Dahm, T., 2012. Sinkholes in the city of Hamburg – New urban shear-wave reflection seismic system enables high-resolution imaging of subsurface structures. *J. Appl. Geophys.* 78, 133–143. <https://doi.org/10.1016/j.jappgeo.2011.02.003>.
- Kujansuu, R., Kurkinen, I., Niemelä, J., 1995. Glaciofluvial deposits in Finland. In: Ehlers, J., Kozarski, S., Gibbard, P.L. (Eds.), *Glacial deposits in North-East Europe*. A.A. Balkema, Rotterdam, The Netherlands, pp. 67–75.
- Kukkonen, M., Stén, C.G., Herola, E., 1993. Loimaan kartta-alueen maaperä. Geological map of Finland. 1:100000. Explanation to the map of Quaternary deposits, sheet 2111. 49 pp. Geological Survey of Finland, Espoo.
- Mäkinen, J., 2003a. Time-transgressive deposits of repeated depositional sequences within interlobate glaciofluvial (esker) sediments in Köyliö, SW Finland. *Sedimentology* 50, 327–360. <https://doi.org/10.1046/j.1365-3091.2003.00557.x>.
- Mäkinen, J., 2003c. Development of depositional environments within the interlobate Säkyliänharju-Virttaankangas glaciofluvial complex in SW Finland. 65 pp. *Ann. Acad. Sci. Fenn. AIII* 165.
- Mäkinen, J., 2004. The sedimentology and depositional history of the Säkyliänharju-Virttaankangas interlobate glaciofluvial complex in SW Finland. 27 p. *Annales Universitatis Turkuensis Ser AII* 173. Painsalama Oy, Turku, Finland.
- Mäkinen, J., Räsänen, M., 2003. Early Holocene regressive spit-platform and nearshore deposition on a glaciofluvial ridge during the Yoldia Sea and the Ancylus Lake Phases of the Baltic Basin, SW Finland. *Sedim. Geol.* 158, 25–56. [https://doi.org/10.1016/S0037-0738\(02\)00240-3](https://doi.org/10.1016/S0037-0738(02)00240-3).
- Malehmir, A., Lindén, O., Friberg, B., Brodic, B., Möller, H., Svensson, M., 2018. Unravelling contaminant pathways through a detailed seismic investigation, Varberg-Southwest Sweden. EAGE 24<sup>th</sup> European meeting of Environmental and Engineering Geophysics. Investigations – High-resolution Engineering Seismic Studies I. <https://doi.org/10.3997/2214-4609.201802610>.
- Maries, G., Ahokangas, E., Mäkinen, J., Pasanen, A., Malehmir, A., 2017. Interlobate esker architecture and related hydrogeological features derived from a combination of high-resolution reflection seismics and refraction tomography, Virttaankangas, SW-Finland. *Hydrogeol. J.* 25, 829–845. <https://doi.org/10.1007/s10040-016-1513-9>.
- Martinez, K., Ploug, C., Pugin, A., Mendoza, J.A., 2010. New three-component landstreamer system developed for groundwater and engineering applications. Extended abstract. *Near Surface 2010 – 16th European Meeting of Environmental and Engineering Geophysics*, P29. Zurich, Switzerland, 6–8 September 2010.
- Mitchum, R.M., Vail, P.R., Sangree, J.B., 1977. Stratigraphic interpretation of seismic reflection patterns in depositional sequences. In: Payton, C.E. (Ed.), *Seismic Stratigraphy – Applications to Hydrocarbon Exploration*. AAPG Memoirs 16, pp. 117–123.
- National Land Survey of Finland, 2016. General map 1: 1000 000. NLS File service of open data. <https://tiedostopalvelu.maanmittauslaitos.fi/tp/kartta?lang=en> (accessed 5 February 2016).
- Oldenborger, G.A., Pugin, A.J.-M., Pullan, S.E., 2013. Airborne time-domain electromagnetics, electrical resistivity and seismic reflection for regional three-dimensional mapping and characterization of the Spiritwood Valley Aquifer, Manitoba, Canada. *N. Surf. Geophys.* 11, 63–74. <https://doi.org/10.3997/1873-0604.2012023>.
- Oldenborger, G.A., Logan, C.E., Hinton, M.J., Pugin, A.J.-M., Sapia, V., Sharpe, D.R., Russell, H.A.J., 2016. Bedrock mapping of buried valley networks using seismic reflection and airborne electromagnetic data. *J. Appl. Geophys.* 128, 191–201. <https://doi.org/10.1016/j.jappgeo.2016.03.006>.
- Pasanen, A., 2009. The application of ground penetrating radar to the study of Quaternary depositional environments. 45 p. *Res Terrae Ser. A* 0358-2477, 27.
- Pilecki, Z., Isakow, Z., Czarny, R., Pilecka, E., Harba, P., Barnaś, M., 2017. Capabilities of seismic and georadar 2D/3D imaging of shallow subsurface of transport route using the Seismobile system. *J. Appl. Geophys.* 143, 31–41. <https://doi.org/10.1016/j.jappgeo.2017.05.016>.
- Pitkäranta, R., 2013. Lithostratigraphy and Age of Pre-late Weichselian Sediments in the Suupohja Area, Western Finland. 66 pp. *Annales Universitatis Turkuensis. Ser. AII* 284. Painsalama Oy, Turku, Finland.
- Pugin, A.J.-M., Pullan, S.E., Sharpe, D.R., 1999. Seismic facies and regional architecture of the Oak Ridges Moraine area, southern Ontario. *Can. J. Earth Sci.* 36, 409–432. <https://doi.org/10.1139/e98-104>.
- Pugin, A.J.-M., Larson, T.H., Sargent, S.L., 2004. Near-surface mapping using SH-wave and P-wave seismic landstreamer data acquisition in Illinois, U.S. *Lead. Edge* 23, 677–682. <https://doi.org/10.1190/1.1776740>.
- Pugin, A.J.-M., Sargent, S.L., Hunt, L., 2006. SH and P-wave seismic reflection using landstreamers to map shallow features and porosity characteristics in Illinois. Extended abstract, CD-ROM edition. 19th SAGEEP Meeting, April 2–6 2006, Seattle, WA, pp. 1094–1109.
- Pugin, A.J.-M., Pullan, S.E., Hunter, J.A., Oldenborger, G.A., 2009a. Hydrogeological prospecting using P- and S-wave landstreamer seismic reflection methods. *N.Surf. Geophys.* 7, 315–327. <https://doi.org/10.3997/1873-0604.2009033>.
- Pugin, A.J.-M., Pullan, S.E., Hunter, J.A., 2009b. Multicomponent high-resolution seismic reflection profiling. *Lead. Edge* 28, 1182–1265. <https://doi.org/10.1190/1.3249782>.
- Pugin, A.J.-M., Pullan, S.E., Duchesne, M., 2013. Regional hydrostratigraphy and insights into fluid flow through a clay aquitard from shallow seismic reflection data. *Lead. Edge* 32, 742–748. <https://doi.org/10.1190/le32070742.1>.
- Pugin, A.J.-M., Oldenborger, G.A., Cummings, D.I., Russell, H.A.J., Sharpe, D.R., 2014. Architecture of buried valleys in glaciated Canadian Prairie regions based on high resolution geophysical data. *Qua. Sci. Rev.* 86, 13–23.
- Pullan, S.E., Pugin, A.J.-M., Hunter, J., 2007. Shallow seismic reflection methods for the delineation and hydrogeological characterization of buried eskers in eastern Ontario: Denver, Colorado. 20th Annual Symposium on the Application of Geophysics to Environmental and Engineering Problems (SAGEEP) Meeting, April 1–5, 2007.
- Punkari, M., 1980. The ice lobes of the Scandinavian ice sheet during the deglaciation in Finland. *Boreas* 9, 307–310. <https://doi.org/10.1111/j.1502-3885.1980.tb00710.x>.
- Russell, H.A.J., Arnott, R.W.C., Sharpe, D.R., 2003. Evidence for rapid sedimentation in a tunnel channel, Oak Ridges Moraine, southern Ontario, Canada. *Sedim. Geol.* 160, 33–55. [https://doi.org/10.1016/S0037-0738\(02\)00335-4](https://doi.org/10.1016/S0037-0738(02)00335-4).
- Salli, I., 1953a. Pre-Quaternary rocks. Geological map of Finland. 1: 100 000. Sheet 2111 Loimaa. Geological Survey of Finland, Espoo.
- Salli, I., 1953b. Explanation to the map of rocks. Geological map of Finland 1: 100 000. Sheet 2111 Loimaa. 41 p. Geological Survey of Finland, Espoo.
- Santos, J.B., 2012. Late Wisconsinan glacial geomorphology of the Kent Interlobate Complex, Ohio, USA. *Finisterra* 47, 65–84. <https://doi.org/10.18055/Finis1258>.
- Sharpe, D.R., Pullan, S.E., Warman, T.A., 1992. A basin analysis of the Wabigoon Area of Lake Agassiz, a Quaternary Clay Basin in Northwestern Ontario. *Geogr. Phys. Quat.* 46, 295–309. <https://doi.org/10.7202/032916ar>.
- Sharpe, D.R., Pugin, A.J.-M., Pullan, S.E., Gorrell, G., 2003. Application of seismic stratigraphy and sedimentology to regional hydrogeological investigations; an example from Oak Ridges Moraine, southern Ontario, Canada. *Can. Geotech. J.* 40, 711–730. <https://doi.org/10.1139/t03-020>.
- Steeple, D.W., Miller, R.D., 1990. Seismic reflection methods applied to engineering and groundwater problems. In: Ward, S.H. (Ed.), *Geotechnical and Environmental Geophysics Volume 1: Review and Tutorial*. Society of Exploration Geophysicists, United States of America, pp. 1–30.
- Thomas, G.S.P., Montague, E., 1997. The morphology, stratigraphy and sedimentology of the Carstairs esker, Scotland, U.K. *Quat. Sci. Rev.* 16, 661–674. [https://doi.org/10.1016/S0277-3791\(97\)00014-0](https://doi.org/10.1016/S0277-3791(97)00014-0).
- Tremblay, T., Hunter, J., Lamontagne, C., Nastev, M., 2010. High resolution seismic survey in a contaminated Esker Area, Chateaugay River Watershed. Quebec. *Can. Water Resour. J.* 35, 417–432. <https://doi.org/10.4296/cwrj3504417>.

- Turku Region Water Ltd, 2016a. The coarse-grained unit. ArcGIS shapefile 1 (3), 2016.
- Turku Region Water Ltd, 2016b. The MAR Plant Area. ArcGIS shapefile 1.3.2016.
- Turku Region Water Ltd, 2016c. The Monitoring Wells. ArcGIS shapefile 1.3.2016.
- Valjus, T., 2006. Turun Seudun Vesi. Pohjavesialueen kallionpinnan tason määrittäminen painovoimamittausten avulla. 41 pp. Geological survey of Finland, Report of Investigation 13.01.2006. Geological Survey of Finland, Espoo.
- Van der Veen, M., Spitzer, R., Green, A.G., Wild, P., 2001. Design and application of a towed landstreamer for cost-effective 2D and pseudo-3D shallow seismic data acquisition. *Geophysics* 66, 482–500. <https://doi.org/10.1190/1.1444939>.
- Vangkilde-Pedersen, T., Dahl, F.J., Ringgaard, J., 2006. Five years of experience with landstreamer vibroseis and comparison with conventional seismic data acquisition. Proceedings of the Symposium on the Application of Geophysics to Engineering and Environmental Problems (SAGEEP'06), Seattle, Washington, USA, 2–6 April 2006, pp. 1086–1093. <https://doi.org/10.4133/1.2923567>.
- Warren, W.P., Ashley, G.M., 1994. Origins of the ice-contact stratified ridges (eskers) of Ireland. *J. Sedim. Res.* A64, 433–449. <https://doi.org/10.1306/D4267DD9-2B26-11D7-8648000102C1865D>.